The inflection point hypothesis: The relationship between the temperature dependence of enzyme catalyzed reaction rates and microbial growth rates

Erica J. Prentice[1], Joanna Hicks[1], Hendrik Ballerstedt[2], Lars M. Blank[2], Liyin L. Liang[3], Louis A. Schipper[1], Vickery L. Arcus[1]*

[1]School of Science, University of Waikato, Hamilton 3216, New Zealand

[2] Institute of Applied Microbiology - iAMB, Aachen Biology and Biotechnology – ABBt, RWTH Aachen University, Worringerweg 1, D-52074 Aachen, Germany

[3] Manaaki Whenua − Landcare Research, Private Bag 11052, Palmerston North 4442, New Zealand

KEYWORDS

Macromolecular rate theory (MMRT), temperature, enzyme catalysis, metabolic pathway, metabolism, growth rates, adaptation

GRAPHICAL ABSTRACT

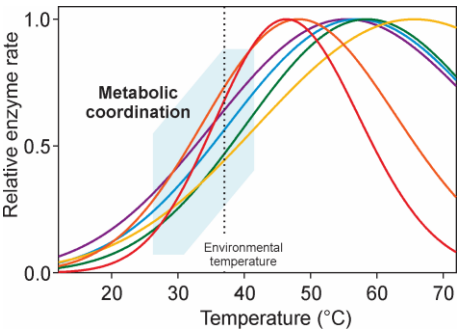

ABSTRACT

The temperature dependence of biological rates at different scales (from individual enzymes, to isolated organisms, to ecosystem processes such as soil respiration and photosynthesis) is the subject of much historical and contemporary research. The precise relationship between the temperature dependence of enzyme rates and those at larger scales is not well understood. We have developed macromolecular rate theory (MMRT) to describe the temperature dependence of biological processes at all scales. Here we formalize the scaling relationship by investigating MMRT at both the molecular scale (constituent enzymes) and for growth of the parent organism. We demonstrate that the inflection point (T_{inf}) for the temperature dependence of individual metabolic enzymes coincides with the optimal growth temperature for the parent organism, and we rationalize this concordance in terms of the necessity for linearly correlated rates for metabolic enzymes over fluctuating environmental temperatures to maintain homeostasis. Indeed, T_{inf} is likely to be under strong selection pressure to maintain coordinated rates across environmental temperature ranges. At temperatures where rates become uncorrelated, we postulate a regulatory catastrophe and organism growth rates precipitously decline at temperatures where this occurs. We show that the curvature in the plots of the natural log of the rate versus temperature for individual

enzymes determines the curvature for the metabolic process overall and the curvature for the temperature dependence of the growth of the organism. We have called this "the inflection point hypothesis" and this hypothesis suggests many avenues of investigation in the future including avenues for engineering organisms' thermal tolerance.

TEXT

Introduction

Biological processes at different scales display a temperature optima (T_{opt}) – the temperature at which the given process is at a maximum. For example, individual enzymes display temperature optima such that enzyme-catalyzed reaction rates drop sharply at temperatures above T_{opt}.[1-2] Similarly, individual organism growth rates show a well-defined T_{opt} value above which rates precipitously decline.[1, 3]. Ecosystem rates such as leaf respiration, photosynthesis, and microbial processes display temperature optima.[4-6] An obvious and much studied question concerns the degree to which the temperature dependence for these various processes are related and many authors have sought relationships between enzyme T_{opt} and organism/ecosystem T_{opt} values. The simplest model which is widely used is the "master enzyme" model that postulates a single metabolic enzyme whose denaturation above a particular temperature dominates the metabolism of its parent organism and whose T_{opt} coincides with the T_{opt} for growth of the parent organism.[3] Models of increasing sophistication have been proposed using, for example, proteome wide analysis of thermal unfolding[7], and genome scale metabolic modelling.[8] Recently, machine learning and Bayesian analysis has been brought to bear on this question.[9] Cell membrane composition is also an important feature of organismal thermotolerance.[10]

We have recently developed macromolecular rate theory (MMRT) to model the temperature dependence of enzyme-catalyzed reaction rates and we have also noted that this model accurately describes the temperature-dependence of organism growth rates and ecosystem rates.[1, 4-5] MMRT invokes an activation heat capacity ($\Delta C_p^{\ddagger}$) that arises from the difference in heat capacity between the enzyme-substrate complex (ES) and the enzyme-transition state complex (E-TS) along the reaction coordinate. The activation heat capacity is a consequence of an enzyme preferentially stabilizing the transition state for the reaction when compared to the substrate (i.e. $K_{d,TS} << K_{d,substrate}$). The activation heat capacity determines the "curvature" seen in a ln(rate) versus T plot and also determines the value of T_{opt} without the need to invoke enzyme denaturation. Furthermore, the curvature seen for most biological processes from growth rates[1], to microbial processes[5] and leaf respiration[4] is well explained with MMRT. However, this raises a further question about the relationship between the curvature and T_{opt} for individual enzymes and that for organism growth and potentially for rates at increasing scales.

Here, we investigate the relationship between the temperature dependence of individual enzymes and that for a metabolic pathway and organism growth using the first six enzymes of the glycolysis pathway individually, together *in vitro*, and *in vivo*. We show that despite individual rates varying by three orders of magnitude, and the enzymes having widely distributed T_m values,[7] the curvature of the temperature dependence for individual enzyme rates all contribute to the curvature of the parent metabolic pathway, and the curvature of the organism growth rate. We propose "the inflection point hypothesis" whereby evolutionary processes place the inflection points for individual enzymes at a common temperature, thus linearly correlating enzyme rates over temperature changes close to the average environmental temperature for the organism. We also conclude that the precipitous decline in organism growth rates at high temperatures are the result

of the loss of correlation between metabolic enzyme rates leading to a regulatory catastrophe for the organism with the buildup of toxic intermediates and dysregulation of critical metabolic processes.

Theoretical framework

In enzyme characterizations, T_{opt} (the temperature of maximum activity, $dk/dT = 0$; Figure 1) is commonly reported as a measure of thermal adaptation, but how relevant is T_{opt} in the context of an organisms' environment? Enzyme T_{opt}'s show a general relationship to growth temperature, with T_{opt} values increasing for enzymes from psychrophiles through to thermophiles.[11] However, enzymatic T_{opt} values are consistently higher than environmental and optimum growth temperatures. This disparity is especially evident for psychrophilic enzymes.[12-14]

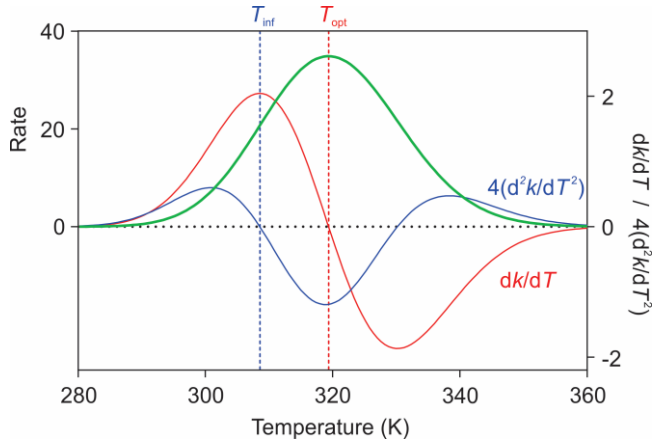

Figure 1. The temperature dependence of enzyme rates (green), along with the first (red) and second (blue) derivatives. T_{opt} ($dk/dT = 0$) and T_{inf} ($d^2k/dT^2 = 0$) are illustrated as vertical dashed lines at the point where the first and second derivative cross zero respectively. The second derivative has been scaled by a factor of four for clarity.

Under "the inflection point hypothesis", we propose that enzymatic T_{opt} is not an evolutionarily selected parameter. Indeed, as T_{opt} is generally above viable growth temperatures, there can be no obvious selective pressure on T_{opt}. Instead, we propose that T_{inf}, the temperature of the lower inflection point of an enzyme's thermal response curve ($d^2k/dT^2 = 0$; Figure 1), is the evolutionarily relevant parameter in enzyme adaptation to temperature. The inflection point is the steepest point of an enzyme thermal response curve, about which rates are approximately linear ($d^2k/dT^2 = 0$ implies zero "curvature" at this point). The relative rates of multiple enzymes with aligned T_{inf} values are robust to changes in temperature about the T_{inf} due to the collinearity of the enzyme rates across these temperatures. Thus by aligning T_{inf} at the average environmental temperature, metabolism has an intrinsic homeostasis over increases and decreases in temperature over short time scales as relative rates through each enzyme scale equally, maintaining relative ratios of metabolic intermediates. In contrast, for other temperature zones of the curves, small changes in temperature result in divergent rate responses of enzymes. We propose that T_{inf} alignment has significance for the temperature response of growth rates, where the loss of coordination at high temperatures is evident in precipitous declines in growth rates.

Methods

Cloning, protein expression and purification

Expression systems for the enzymes glucokinase (GK; EC 2.7.1.2), phosphoglucose isomerase (PGI; EC 5.3.1.9), phosphofructokinase I (PFK; EC 2.7.1.11), fructose bisphosphate aldolase II (FBPA; EC 4.1.2.13), triosephosphate isomerase (TPI; EC 5.3.1.1) and glyceraldehyde phosphate dehydrogenase (GAPD; EC 1.2.1.12) from *Escherichia coli* BL21 Gold (DE3) were cloned into

pPROEX HtB in *E. coli* DH5α. Protein expression was induced in mid-exponential phase with 1 mM IPTG at 37 °C either in LB media overnight (GK, PFK, FBPA, and TPI), or in LB with 2 $g.L^{-1}$ glucose over four hours (PGI, and GAPD). Proteins were purified by immobilized metal ion affinity chromatography in 50 mM HEPES, pH 7.4, 150 mM NaCl over a 20 $mM.ml^{-1}$ imidazole gradient (20-1000 mM), followed by gel filtration chromatography (50 mM HEPES, pH 7.4, 150 mM NaCl).

Kinetic characterizations

Enzyme assays were performed in 50 mM HEPES, pH 7.4 (intercellular pH of *E. coli)*[15], 150 mM NaCl, 10 mM $MgCl_2$, and 2.5 mM $(NH_4)_2SO_4$ in a Heλios γ spectrophotometer (Thermo Fisher Scientific) coupled to single cell peltier temperature control. Temperature profiles for each enzyme were performed at saturating substrate conditions, as determined by Michaelis Menten characterizations at 37 and 44-45 °C (Supplementary Figure S1). Reaction components were brought to temperature prior to reaction initiation by the addition of enzyme. Initial rates of reaction were measured over ten seconds to reduce possible confounding effects from denaturation, especially at high temperatures. Reactions were monitored continuously at 340 nm following the production of NAD(P)H. Specifically, GK was characterized in a coupled reaction with glucose-6-phosphate dehydrogenase to produce NADPH.[16] PGI was assayed in reverse, forming glucose-6-phospahte to allow detection coupled to glucose-6-phosphate dehydrogenase.[17] PFK was assayed in a coupled reaction with FBPA and GAPD for continuous detection of NADH production.[18] FBPA [19] and TPI [20] reactions were coupled to the reduction of NAD^+ by GAPD, while GAPD activity was measured directly by product NADH formation.[21] For full characterisation component details, see Supplementary Table S1.

The pathway was assayed at saturating concentrations of ligands NAD^+, ATP, and P_i. Starting substrate, glucose or glucose-6-phosphate, was added at saturating concentrations for GK and PGI respectively, and the reaction followed at 340 nm by the production of NADH by GAPD at the pathway endpoint (full assay details in Supplementary Table S1).

Temperature profiles for both individual enzymes and pathways were fit with equation 1 in GraphPad Prism (GraphPad Software, La Jolla California USA, www.graphpad.com), where k_B is the Boltzmann constant, h is Planck's constant, R is the ideal gas constant, T is temperature in Kelvin, $\Delta H^{\ddagger}_{T_0}$ and $\Delta S^{\ddagger}_{T_0}$ are the enthalpy and entropy change over the reaction at the reference temperature (T_0), respectively. The reference temperature was set at four degrees below the temperature at which maximum rates were measured, consistent with the literature.[5] T_{opt} and T_{inf} were calculated via equations 2 and 3 respectively from best fit values determined in equation 1:

$$\ln(k) = \ln\left(\frac{k_B T}{h}\right) - \frac{\left[\Delta H^{\ddagger}_{T_0} + \Delta C_p^{\ddagger}(T - T_0)\right]}{RT} + \frac{\left[\Delta S^{\ddagger}_{T_0} + \Delta C_p^{\ddagger} \ln\left(\frac{T}{T_0}\right)\right]}{R} \quad (1)$$

$$T_{opt} = \frac{\Delta H^{\ddagger}_{T_0} - \Delta C_p^{\ddagger}.T_0}{-\Delta C_p^{\ddagger} - R} \sim T_0 - \frac{\Delta H^{\ddagger}_{T_0}}{\Delta C_p^{\ddagger}} \quad (2)$$

$$T_{inf} = \frac{\Delta H^{\ddagger}_{T_0} - \Delta C_p^{\ddagger}.T_0}{-\Delta C_p^{\ddagger} + \sqrt{-\Delta C_p^{\ddagger}.R}} \quad (3)$$

Pathway modelling

To further investigate the metabolic pathway, reaction rates were modelled in two ways from the measured k_{cat} variation with temperature (Figure 2) and experimental enzyme concentrations

(Supplementary Table S1). First, the theoretical pathway rate at each temperature (k_{tot}) was calculated via equation 4, where overall pathway rates are dependent on the inverse turnover time of each enzymatic step ($\frac{1}{k_1}$ etc.):

$$\frac{1}{k_{tot}} = \frac{1}{k_1} + \frac{1}{k_2} + \cdots \frac{1}{k_n} \quad (4)$$

Secondly, to account for changing component concentrations and the effect of sub-saturating substrates, the pathway was also modelled using CellML[22] to incorporate enzyme Michaelis Menten behavior. Binding constants at 37 °C and variation in k_{cat} with temperature were taken from experimental determinations (Supplementary Figure S1 and Figure 2 respectively). Due to the short experimental assay period favoring the forward reaction, enzymes with reversible reactions (except TPI) were simplified to allow the forward reaction only. Due to the fast and reversible nature of TPI at the pathway branch point, the triose pool components (dihydroxyacetone phosphate and glyceraldehyde-3-phosphate) were modelled via an equilibrium constant, consistent with treatment in the literature.[23] Substrate concentrations were set to model the experimental system set up (Supplementary Table S1). The model is available online at the CellML Model Repository (models.cellml.org/cellml)

E. coli growth rates

E. coli BL21 (DE3) growth rates were measured in M9 minimal media[24] containing either 0.4 % (w/v) glucose or glucose-6-phosphate as the sole carbon source. Cultures were inoculated 1 in 100 from stationary phase cultures grown in M9 glucose. Growth rates were calculated by measuring backscatter via a Cell Growth Quantifier (aquila biolabs, Baesweiler, Germany) using 25 ml growth medium in 250 ml flasks with shaking at 200 rpm.

Results and discussion

Enzyme adaptation to environmental temperature

For the six enzymes from the glycolytic pathway of *E. coli* characterized here using MMRT, it is evident that T_{opt} values are not only consistently greater than optimal growth temperature (37 °C, 310.15 K), but highly variable between enzymes. Characterized T_{opt} values range from nine to 29 degrees above the optimal growth temperature (average 328.2 K, standard deviation 7.1 K; Figure 2). There is however a close correlation between optimal growth temperature and the lower inflection point for the enzyme MMRT curve (T_{inf}; Figures 2 and 3). For the six enzymes studied, T_{inf} values have an average value of 310.3 ± 3.2 K, clustering around the optimum growth temperature of 310.15 K (Figure 3). From this concordance, we argue that T_{inf} presents a more informative parameter for linking *in vitro* enzyme characterizations to bacterial growth temperatures (when compared to T_{opt}), and is an association which warrants investigation in further species.[25]

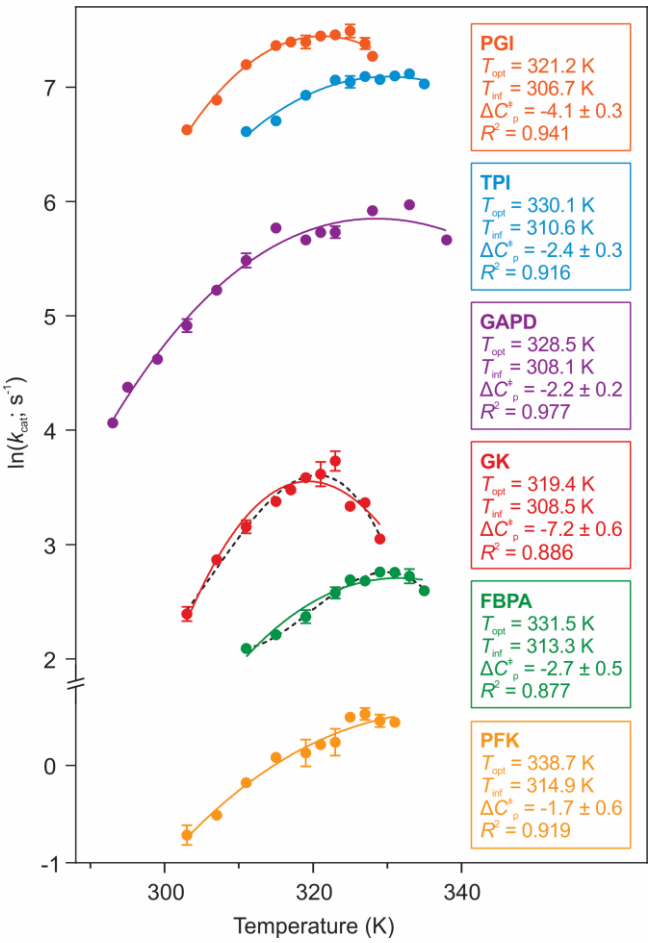

Figure 2. Temperature-rate data for the first six enzymes of the glycolytic pathway from *E. coli*. Data shown are the initial rates of reaction (at saturating substrate), fitted to equation 1. Data are given as the mean; error bars, where visible, represent the SD of three replicates (with the exception of T = 328-338 K for GAPD, as single measures). $\Delta C_p^{\ddagger}$ values are in kJ.mol^{-1}.K^{-1} ± SE. T_{opt} and T_{inf} values are calculated from equations 2 and 3 respectively. Data for GK and FBPA exhibit non-random deviations from equation 1, and these data are better fit using a temperature dependent $\Delta C_p^{\ddagger}$ (dotted lines, F test p-value 0.0028 and < 0.0001 respectively, see Supplementary for further details). For simplicity of modelling, temperature independent MMRT (equation 1) was used subsequently in all cases.

If temperature rate profiles for enzymes shift over evolutionary time to place T_{inf} at the environmental temperature, this suggests that there exists a selection pressure on T_{inf}. We propose that fixing T_{inf} at the average environmental temperature (37 °C for *E. coli*) serves as a mechanism for tightly coordinating the relative rates of enzyme activity across cellular metabolism over short time-scale fluctuations in environmental temperature. Enzymes do not evolve in isolation, but as components of metabolic networks and within a framework of regulatory controls, to modulate activity both within and between pathways, in the context of environmental conditions.[26-27] Metabolic networks have been found to enact high levels of intrinsic self-regulation, where feedback regulation and effector systems rapidly and passively adjust enzyme activities, as opposed to active hierarchical control from transcriptional, translational and post-translational modifications.[28] The metabolic-wide alignment of T_{inf} values to the environmental temperature functions as a further means of instantaneous intrinsic metabolic coordination, allowing passive synchronization of enzyme activities over short time-scale fluctuations in environmental temperature. This coordination is due to the linearly correlated rates of different enzymes about the inflection point (Figure 3). By coordinating T_{inf} values at the average environmental temperature, relative rates through each enzyme in the pathway scale equally over both increases and decreases in temperature, maintaining the ratios of metabolic intermediates (i.e. homeostasis).

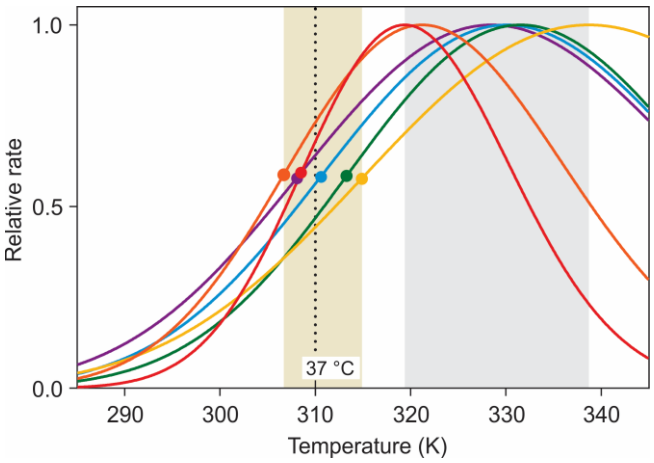

Figure 3. Relative temperature profiles of glycolytic enzymes from *E. coli*. The fit of equation 1 to the data (Figure 2) is shown for each enzyme. Inflection points for each enzyme are indicated as circles; the temperature span of T_{inf} values is shaded in yellow. By comparison, the range of T_{opt} values is shaded in grey. The optimum growth temperature of *E. coli* (37 °C) is indicated with a dotted line.

The significance of T_{inf}

The observed alignment of T_{inf} at the environmental temperature immediately raises the question as to why T_{inf} is aligned at this temperature rather than T_{opt}? First, coordinating T_{inf} values demands less precise alignment of temperature profiles than the coordination of T_{opt}. Due to the approximately linear relationship between rate and temperature about the inflection point ($d^2k/dT^2 = 0$), T_{inf} values do not need to be precisely matched to preserve relative rates over temperature variations. By comparison, if rates were to be coordinated about T_{opt} (where curvature is at a maximum, Figure 1), stricter alignment is necessary to achieve rate coordination between enzymes due to the steep declines in rate either side of T_{opt}.

In addition, if T_{opt} were lowered to match environmental temperatures, this would have consequences for enzyme kinetics and temperature sensitivity. There is a defined relationship between T_{opt} and $\Delta C_p^{\ddagger}$ where decreases in T_{opt} can only be achieved via more negative $\Delta C_p^{\ddagger}$ values.[1] The first consequence of this is the "psychrophilic trap", whereby increasingly negative $\Delta C_p^{\ddagger}$ values impose increasing curvature and much greater temperature sensitivity.[29] Thus, shifting T_{opt} down to the environmental temperature also steepens curvature about T_{opt}, incurring a higher penalty of rate reductions with changes to lower temperatures. The molecular strategies of decreasing $\Delta C_p^{\ddagger}$ (as evident in psychrophilic enzymes)[30] involve increases in the heat capacity (C_p) for the enzyme-substrate complex (more flexible) and/or decreases in C_p of the enzyme transition state species (more rigid).[29] Our hypothesis is that fixing of T_{inf} instead of T_{opt} achieves two things: one, linearly correlated rates for multiple metabolic enzymes over small fluctuations in temperature, and two, escaping the detrimental consequences of greater curvature (temperature sensitivity) incurred by lowering T_{opt}.

The temperature dependence of growth rates

Enzyme kinetic parameters are often considered in isolation, yet this misses vital information pertaining to function within a metabolic context.[31] To investigate how the different temperature profiles of the characterized glycolytic enzymes contribute to the temperature dependence of a metabolic pathway, the six enzymes were characterized as a pathway in a one-pot reaction (Figure 4A). Pathway reaction rates measured the rate of production of 1,3-bisphosphoglycerate from glucose, dependent on six enzymatic steps.

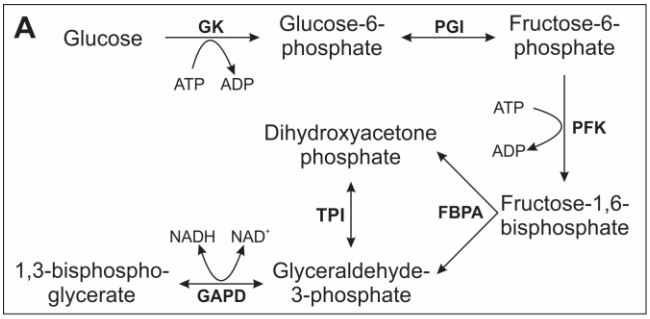

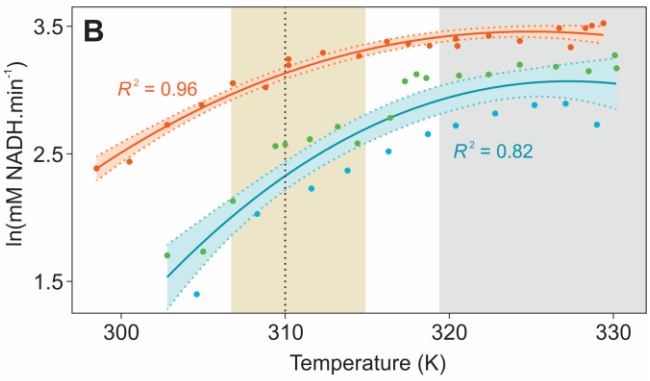

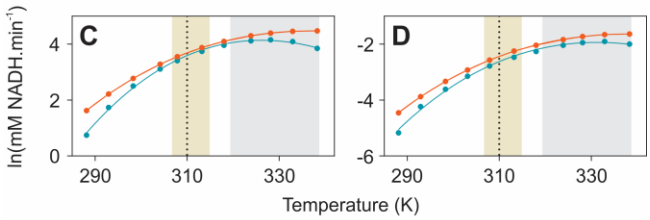

E	*Experimental pathway (B)*	*No substrate limitation (C)*	*Substrate limitation (D)*
Five steps	T_{opt} = 324.9 K T_{inf} = 305.9 K $\Delta C^{\ddagger}_p$ = -2.4 (3)	T_{opt} = 345.8 K T_{inf} = 322.6 K $\Delta C^{\ddagger}_p$ = -1.85 (1)	T_{opt} = 346.9 K T_{inf} = 323.0 K $\Delta C^{\ddagger}_p$ = -1.75 (2)
Six steps	T_{opt} = 327.3 K T_{inf} = 312.6 K $\Delta C^{\ddagger}_p$ = -4 (1)	T_{opt} = 335.2 K T_{inf} = 318.7 K $\Delta C^{\ddagger}_p$ = -3.4 (1)	T_{opt} = 340.3 K T_{inf} = 320.8 K $\Delta C^{\ddagger}_p$ = -2.5 (2)

Figure 4. The temperature dependence of the glycolytic pathway. **(A)** Enzymes and substrates/products of the characterized pathway. **(B)** Experimental determination of the temperature dependence of a five- and six-step pathway. Data are presented as single points, with the 95 % confidence interval of fitting indicated by shading. Pathway rates were detected by the formation of NADH from glucose-6-phosphate and glucose, respectively. For the six-step pathway, data is separated based on a temporal delay in the enzyme mixture equilibration time

(blue and green) which resulted in an increased rate over time. These data are fitted as one data set (turquoise). **(C)** and **(D)** Modelling of the pathway rates without and with incorporation of substrate limitations, respectively. R^2 values for modelled data are 1.00 in all cases. **(E)** Fit parameters for experimental and modelled data. $\Delta C_p^{\ddagger}$ values are in kJ.mol^{-1}.K^{-1}; the standard error of fitting for the last significant figure is given in brackets. T_{opt} and T_{inf} values were calculated from equations 2 and 3 respectively.

The temperature dependence of the one-pot reaction of six pathway enzymes has an observed curvature ($\Delta C_{p,obs}^{\ddagger}$) of -4 ± 1 kJ.mol^{-1}.K^{-1}. Pathway data (Figure 4B) are color coded into two replicates differing only in the period over which enzymes were combined prior to the assay (on the scale of hours). Intriguingly, rates increased with increasing incubation time suggesting that some form of coordination is occurring over longer time periods. This would be consistent with the formation of supercomplexes, as has been observed previously with glycolytic enzymes.[32] However, this is purely speculative at this juncture and is the subject of ongoing investigations. Nonetheless, faster rates in the latter collected data set confirm no system degradation occurred over the experimental time frame and that the observed curvature is reproducible.

Emphasis is commonly placed on rate-determining steps as dominating overall rates and temperature responses in metabolic processes. For example, models by Corkrey[3] incorporate a single rate limiting master enzyme restraining rates below T_{opt}, while declines above T_{opt} are simplified to denaturation of this key enzyme. If this were the case, we would expect PFK, as the rate limiting enzyme across all temperatures to be the main contributor to curvature of pathway rates. Contrary to this expectation, the measured pathway curvature is greater than that of PFK

($\Delta C^{\ddagger}_{p,obs}$ = -4 ± 1 and $\Delta C^{\ddagger}_{p}$ = -1.7 ± 0.6 kJ.mol^{-1}.K^{-1} respectively). This suggests an influence from the remaining enzymes with more negative $\Delta C^{\ddagger}_{p}$ values in constraining the curvature to a greater extent than PFK alone. As the first step of the pathway (GK) is highly temperature dependent ($\Delta C^{\ddagger}_{p}$ = -7.2 kJ.mol^{-1}.K^{-1}) compared to the remainder of the enzymes (average $\Delta C^{\ddagger}_{p}$ = -2.6 kJ.mol^{-1}.K^{-1}), removal of this step allowed experimental investigation of the contributions of a non-rate limiting pathway enzyme. Removal of the GK catalyzed step reduces the curvature for the conversion of glucose-6-phosphate to 1,3-bisphosphoglycerate, with a measured $\Delta C^{\ddagger}_{p,obs}$ = -2.4 ± 0.3 kJ.mol^{-1}.K^{-1} (Figure 4B). The measurable effect of the removal of GK, a non-rate limiting step, implicates effects from all contributing enzymes on both pathway rates and temperature dependence.

The temperature dependence of the five- and six-enzyme one-pot reactions were further explored by modelling the pathway at substrate saturating and substrate limiting concentrations using equation 4 and CellML, seperately. Modelling under substrate limiting conditions captured the decreasing concentrations of substrate through the pathway to include the effect of enzyme rates below k_{cat}. This is significant in capturing the low substrate concentrations in both the *in vitro* pathway, and in cellular metabolism (Supplementary Figure S2). Both approaches correctly model the relative differences in temperature dependent curvature of the pathway with and without the inclusion of GK (Figure 4C-E). The ability to predict pathway curvature without inclusion of sub-saturating substrate concentration effects indicates curvature is independent of enzymatic rates less than k_{cat}. This agreement between theoretical and experimental approaches for the temperature response of metabolic pathways demonstrates that pathway curvature is sensitive to the curvature

of all the individual enzymes on the pathway, irrespective whether they constitute the rate-determining step.

In vitro pathway rates do not capture the effects of loss of intrinsic coordination at elevated temperatures that become a detrimental factor for growth rates, as postulated earlier from the observed congruence in T_{inf} values (Figure 3). Pathway T_{opt} values are similar to that of individual enzymes, both of which are greater than ten degrees above the optimal growth temperature of *E. coli*. The detrimental effect of this loss of coordination at elevated temperatures is evident in the temperature dependence of *E. coli* growth, as a sudden sharp decrease in rates above 40 ºC (Figure 5A and B). It is significant that the optimal growth temperature for *E. coli* growth is lower than both the optima of the six characterized enzymes and the optima of the one-pot pathway reactions. The precipitous decline in growth rate coincides with the upper end of the range of enzymatic T_{inf} values. We hypothesize that the loss of intrinsic coordination of contributing enzyme rates (above the T_{inf} temperature range) leads to a regulatory catastrophe and this is one of the dominant factors for the decline in growth rates above 40 ºC. Small increases in temperature above T_{inf} are postulated to induce an array of detrimental consequences for cells, including effects such as the buildup and depletion of intermediate chemicals either side of errantly fast or slow enzymes, including toxic intermediates.

The extent of metabolic coordination requires two criteria to be satisfied. The first is that rates are colinear with changes in temperature and this is achieved when $d^2k/dT^2 = 0$, i.e. the inflection point. The second criteria is that the variance in curvature is minimized – that is, the variance in d^2k/dT^2 calculated across the different enzymes is at a minimum (Figure 5C). Notably, variance reaches a maximum as temperatures approach enzymatic T_{opt}, a peak which coincides with

precipitous decreases in growth rates as the cells' ability to regulate diverging enzyme rates is overwhelmed (Figure 5B).

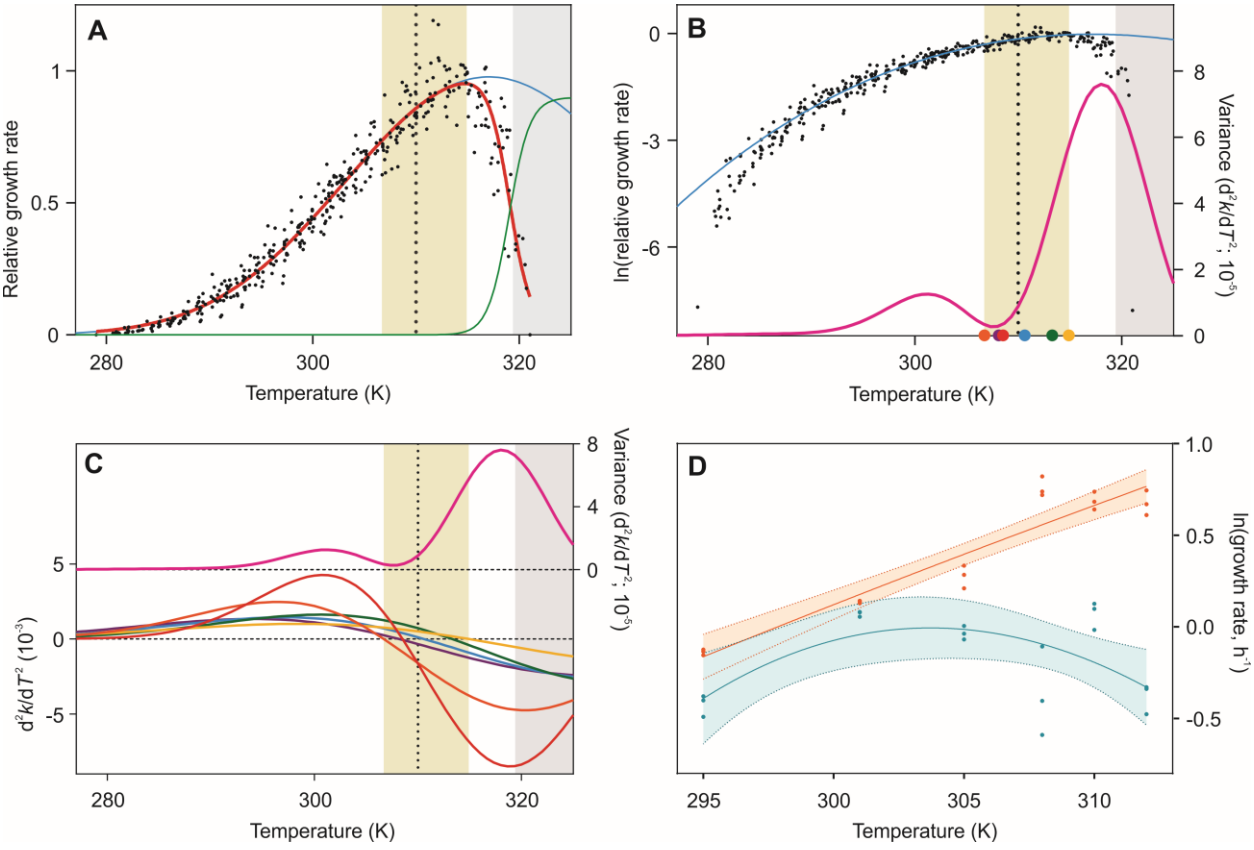

Figure 5. The temperature dependence of microorganism growth rates. The ranges of T_{inf} and T_{opt} for the glycolytic enzymes are given as shaded tan and grey zones respectively. **(A)** Scaled growth rates for a range of *E. coli* strains,[3] fit with MMRT (blue), in conjunction with a (theoretical) "two-state regulatory failure" at high temperatures (green), to give the overall fit (red). The overall fit follows MMRT to 315 K, at which point growth rates rapidly decrease due to a loss of metabolic coordination. **(B)** Growth rates on a log scale to illustrate deviations from MMRT. The variance of d^2k/dT^2 is plotted, showing the congruence between high temperature decreases in rate and the peak in reduced metabolic coordination. Inflection points of the individual enzymes are given as dots. **(C)** The second derivative (d^2k/dT^2) of six glycolytic enzyme rates (colors as in

Figure 1 and 2), and the variance of these functions (mauve). Metabolic coordination is inversely related to the variance of d^2k/dT^2. **(D)** Temperature dependence of *E. coli* growth on glucose and glucose-6-phosphate as the sole carbon source. Individual replicate data is plotted, with the 95 % confidence interval of fitting indicated by shading. Data is fit with MMRT (equation 1). As no curvature is present in G-6-P data, $\Delta C_p^{\ddagger}$ is constrained to zero (i.e. an Arrhenius function).

Given the measurable effects observed at the metabolic level for the glycolytic pathway function with and without GK, we tested the temperature dependence of *E. coli* growth rates under the same conditions using continuous monitoring over time of biomass concentration by light scattering from shake flasks (Figure 5D). We observed significant effects on the temperature dependence of growth when G-6-P is provided as the sole carbon source when compared to glucose. Growth on G-6-P results in faster growth rates (as predicted by our *in vitro* models and one-pot reactions) and a markedly less curved temperature response compared to growth on glucose. The direction of these effects are commensurate with that expected from the metabolic level. However, the extent of the reduction in curvature indicates there are effects additional to the chemical elimination of GK across the *E. coli* metabolism.

Overall, the growth rates of *E. coli* over the temperature range 288-315 K are well modelled by MMRT, where curvature is a function of the combined curvature from contributing metabolic enzymes. Curvature over this range ($\Delta C_{p,obs}^{\ddagger} = -5.7$ kJ.mol^{-1}.K^{-1}) is commensurate with that seen in the glycolytic pathway *in vitro* reflecting the contributions from all enzymes in the pathway. As temperatures extend outside of this range, intrinsic metabolic coordination achieved by aligning

T_{inf} values is lost, resulting in a dysfunctional network, causing catastrophic decreases in growth rates.

Conclusions

Enzymes drive organism growth and ecosystem function, and are a critical component to our understanding of how organisms and populations respond to temperature. Here, the inflection point of six enzyme temperature-rate profiles has been found to closely match the optimal organism growth temperature for *E. coli*, in contrast to the often cited enzymatic T_{opt}. This is consistent with previous observations that enzymatic T_{opt} values are consistently higher than environmental and optimal growth temperatures, and suggests T_{inf} as a more important biological parameter than T_{opt}. We postulate the "inflection point hypothesis", whereby the fixing of enzymatic T_{inf} at the mean environmental temperature for the parent organism achieves coordinated relative enzyme rates over fluctuating temperatures. This coordination in rates maintains relative enzyme rates and metabolic intermediate concentrations over short time scale environmental temperature changes. Fixing T_{inf} reduces the requirement for energy and resource use for active regulatory control of enzyme activates, providing a strong selection pressure for evolution.

In addition, we have shown that the temperature dependent properties of each enzyme in a particular pathway influence the temperature dependence of the whole pathway. This is in contrast to a rate limiting step dominating the pathway behavior. This bridges the gap between enzyme and organism responses to temperature, and we suggest that the observed curvature for the organism,

$\Delta C^{\ddagger}_{\mathrm{p,obs}}$, is a function of the $\Delta C^{\ddagger}_{\mathrm{p}}$ values for the contributing enzymes. Up to the optimal growth temperature for an organism, curvature in growth rates is dictated by the average curvature of contributing metabolic enzymes, with maximal metabolic coordination and growth rates gained over a temperature range about enzymatic T_{inf} where relative enzyme rates scale equally. Above this temperature range where relative rates begin to diverge, a loss of intrinsic metabolic coordination causes a regulatory collapse and severely compromised organism growth rates at high temperatures.

ASSOCIATED CONTENT

UniProt Accession ID for GK (ECBD_1284), PGI (ECBD_4012), PFK (ECBD_4108), FBPA (ECBD_0813), TPI (ECBD_4105), GAPD (ECBD_2224).

Supporting Information.

The following files are available free of charge.

Details for fitting the temperature dependent $\Delta C^{\ddagger}_{\mathrm{p}}$, enzyme assay set up details, and Michaelis Menten characterization data (PDF).

AUTHOR INFORMATION

Corresponding Author

* Email: vic.arcus@waikato.ac.nz

Funding Sources

EJP was supported through this project by the University of Waikato Ph.D. and Graduate Women Educational Trust scholarships. The project was funded by the Marsden Fund of New Zealand (16-UOW-27).

Notes

The authors declare no competing financial interests.

ACKNOWLEDGMENT

We would like to thank Ross Corkrey (Tasmanian Institute of Agriculture) for kindly supplying the previously published *E. coli* growth rate data set.

ABBREVIATIONS

MMRT, Macromolecular Rate Theory; $\Delta C_p^{\ddagger}$, activation heat capacity; T_{opt}, optimum temperature for a process; T_{inf}, lower inflection point of a MMRT curve; GK, glucokinase; PGI, phosphoglucose isomerase; PFK, phosphofructokinase; FBPA, fructose bisphosphate aldose; TPI, triosephosphate isomerase; GAPD, glyceraldehyde phosphate dehydrogenase:.

REFERENCES

(1) Hobbs, J. K., Jiao, W., Easter, A. D., Parker, E. J., Schipper, L. A., and Arcus, V. L. (2013) Change in heat capacity for enzyme catalysis determines temperature dependence of enzyme catalyzed rates, *ACS Chemical Biology 8*, 2388–2393.
(2) Daniel, R. M., and Danson, M. J. (2010) A new understanding of how temperature affects the catalytic activity of enzymes, *Trends in Biochemical Sciences 35*, 584-591.
(3) Corkrey, R., Olley, J., Ratkowsky, D., McMeekin, T., and Ross, T. (2012) Universality of thermodynamic constants governing biological growth rates, *PLoS ONE 7*, e32003.
(4) Liang, L. L., Arcus, V. L., Heskel, M. A., O'Sullivan, O. S., Weerasinghe, L. K., Creek, D., Egerton, J. J. G., Tjoelker, M. G., Atkin, O. K., and Schipper, L. A. (2017) Macromolecular rate theory (MMRT) provides a thermodynamics rationale to underpin the convergent temperature response in plant leaf respiration, *Global Change Biology 24*, 1538-1547.
(5) Schipper, L. A., Hobbs, J. K., Rutledge, S., and Arcus, V. L. (2014) Thermodynamic theory explains the temperature optima of soil microbial processes and high Q_{10} values at low temperatures, *Global Change Biology 20*, 3578–3586.

(6) Kruse, J., Adams, M. A., Kadinov, G., Arab, L., Kreuzwieser, J., Alfarraj, S., Schulze, W., and Rennenberg, H. (2017) Characterization of photosynthetic acclimation in *Phoenix dactylifera* by a modified Arrhenius equation originally developed for leaf respiration, *Trees 31*, 623-644.
(7) Leuenberger, P., Ganscha, S., Kahraman, A., Cappelletti, V., Boersema, P. J., von Mering, C., Claassen, M., and Picotti, P. (2017) Cell-wide analysis of protein thermal unfolding reveals determinants of thermostability, *Science 355*, eaai7825.
(8) Förster, J., Famili, I., Fu, P., Palsson, B. Ø., and Nielsen, J. (2003) Genome-scale reconstruction of the *Saccharomyces cerevisiae* metabolic network, *Genome research 13*, 244-253.
(9) Li, G., Hu, Y., Wang, H., Zelezniak, A., Ji, B., Zrimec, J., and Nielsen, J. (2020) Bayesian genome scale modelling identifies thermal determinants of yeast metabolism, *bioRxiv, doi: 10.1101/2020.04.01.019620*.
(10) Lam, F. H., Ghaderi, A., Fink, G. R., and Stephanopoulos, G. (2014) Engineering alcohol tolerance in yeast, *Science 346*, 71-75.
(11) Elias, M., Wieczorek, G., Rosenne, S., and Tawfik, D. S. (2014) The universality of enzymatic rate–temperature dependency, *Trends in Biochemical Sciences 39*, 299-305.
(12) Peterson, M. E., Eisenthal, R., Danson, M. J., Spence, A., and Daniel, R. M. (2004) A new intrinsic thermal parameter for enzymes reveals true temperature optima, *Journal of Biological Chemistry 279*, 20717-20722.
(13) Thomas, T. M., and Scopes, R. K. (1998) The effects of temperature on the kinetics and stability of mesophilic and thermophilic 3-phosphoglycerate kinases, *Biochemical Journal 330*, 1087-1095.
(14) Lee, C. K., Daniel, R. M., Shepherd, C., Saul, D., Cary, S. C., Danson, M. J., Eisenthal, R., and Peterson, M. E. (2007) Eurythermalism and the temperature dependence of enzyme activity, *FASEB Journal 21*, 1934-1941.
(15) Wilks, J. C., and Slonczewski, J. L. (2007) pH of the cytoplasm and periplasm of *Escherichia coli*: rapid measurement by green fluorescent protein fluorimetry, *Journal of Bacteriology 189*, 5601-5607.
(16) Miller, B. G., and Raines, R. T. (2004) Identifying latent enzyme activities: substrate ambiguity within modern bacterial sugar kinases, *Biochemistry 43*, 6387-6392.
(17) Hansen, T., Wendorff, D., and Schönheit, P. (2004) Bifunctional phosphoglucose/phosphomannose isomerases from the archaea *Aeropyrum pernix* and *Thermoplasma acidophilum* constitute a novel enzyme family within the phosphoglucose isomerase superfamily, *Journal of Biological Chemistry 279*, 2262-2272.
(18) Galzigna, L., Manani, G., Giron, G. P., and Burlina, A. (1977) Enzymatic assay of fructose-1,6-diphosphate for the measurement of its utilization by tissues, *International Journal for Vitamin and Nutrition Research 47*, 88-91.
(19) Nicholas, P. C. (1988) Determination of fructose-1,6-diphosphate aldolase activity with glyceraldehyde-3-phosphate dehydrogenase and diformazan formation, *Biochemical Society Transactions 16*, 753-754.
(20) Sullivan, B. J., Durani, V., and Magliery, T. J. (2011) Triosephosphate isomerase by consensus design: dramatic differences in physical properties and activity of related variants, *Journal of Molecular Biology 413*, 195-208.
(21) Eyschen, J., Vitoux, B., Marraud, M., Cung, M. T., and Branlant, G. (1999) Engineered glycolytic glyceraldehyde-3-phosphate dehydrogenase binds the *anti* conformation of NAD^+

nicotinamide but does not experience A-specific hydride transfer, *Archives of Biochemistry and Biophysics 364*, 219-227.
(22) Yu, T., Lloyd, C. M., Nickerson, D. P., Cooling, M. T., Miller, A. K., Garny, A., Terkildsen, J. R., Lawson, J., Britten, R. D., Hunter, P. J., and Nielsen, P. M. F. (2011) The Physiome Model Repository 2, *Bioinformatics 27*, 743-744.
(23) Teusink, B., Passarge, J., Reijenga, C. A., Esgalhado, E., van der Weijden, C. C., Schepper, M., Walsh, M. C., Bakker, B. M., van Dam, K., Westerhoff, H. V., and Snoep, J. L. (2000) Can yeast glycolysis be understood in terms of *in vitro* kinetics of the constituent enzymes? Testing biochemistry, *European Journal of Biochemistry 267*, 5313-5329.
(24) Anonymous (2010) M9 minimal medium (standard), *Cold Spring Harbor Protocols 2010*.
(25) Gaucher, E. A., Govindarajan, S., and Ganesh, O. K. (2008) Palaeotemperature trend for Precambrian life inferred from resurrected proteins, *Nature 451*, 704-708.
(26) Schlosser, G. (2002) Modularity and the units of evolution, *Theory in Biosciences 121*, 1-80.
(27) Seshasayee, A. S. N., Fraser, G. M., Babu, M. M., and Luscombe, N. M. (2009) Principles of transcriptional regulation and evolution of the metabolic system in *E. coli*, *Genome Research 19*, 79-91.
(28) Millard, P., Smallbone, K., and Mendes, P. (2017) Metabolic regulation is sufficient for global and robust coordination of glucose uptake, catabolism, energy production and growth in *Escherichia coli*, *PLoS Computational Biology 13*, e1005396.
(29) Arcus, V. L., Prentice, E. J., Hobbs, J. K., Mulholland, A. J., van der Kamp, M. W., Pudney, C. R., Parker, E. J., and Schipper, L. A. (2016) On the temperature dependence of enzyme-catalyzed rates, *Biochemistry 55*, 1681-1688.
(30) Feller, G. (2013) Psychrophilic enzymes: from folding to function and biotechnology, *Scientifica 2013*, 512840.
(31) Davidi, D., Longo, L. M., Jabłońska, J., Milo, R., and Tawfik, D. S. (2018) A bird's-eye view of enzyme evolution: chemical, physicochemical, and physiological considerations, *Chemical Reviews 118*, 8786-8797.
(32) Menard, L., Maughan, D., and Vigoreaux, J. (2014) The structural and functional coordination of glycolytic enzymes in muscle: evidence of a metabolon?, *Biology 3*, 623-644.